

# Morphology, Nonisothermal Crystallization Behavior, and Kinetics of Poly(phenylene sulfide)/Polycarbonate Blend

Defeng Wu, Yisheng Zhang, Ming Zhang, Lanfeng Wu

School of Chemistry and Chemical Engineering, Yangzhou University, Yangzhou, Jiangsu, 225002, People's Republic of China

Received 13 November 2006; accepted 16 December 2006

DOI 10.1002/app.26096

Published online 2 April 2007 in Wiley InterScience (www.interscience.wiley.com).

**ABSTRACT:** The morphology and nonisothermal crystallization behavior of blends made of poly(phenylene sulfide) (PPS), with an amorphous polycarbonate (PC) were studied. The blend is found to be partially miscible by the dynamic mechanical thermal analysis (DMTA) and melt rheological measurements. The nonisothermal crystallization behavior of blend was studied by differential scanning calorimetry (DSC). The results show clearly that the crystallization temperatures of PPS component in the blend decrease with increasing of PC contents. The crystallization kinetics was then analyzed by Avrami, Jeziorny, and Ozawa methods. It can be concluded that the addition of

PC decreases the PPS overall crystallization rate because of the higher viscosity of PC and/or partial miscibility of blend, despite of small heterogeneous nucleation effect by the PC phase and/or phase interface. The results of the activation energy obtained by Kissinger method further confirm that the amorphous PC in the partial miscible PPS/PC blend may act as a crystallization inhibitor of PPS. © 2007 Wiley Periodicals, Inc. *J Appl Polym Sci* 105: 739–748, 2007

**Key words:** poly(phenylene sulfide); polycarbonate; blends; nonisothermal crystallization; morphology

## INTRODUCTION

Poly(phenylene sulfide) (PPS) is a semicrystalline polymer that has been increasingly used as an engineering thermoplastic with dual properties of thermoplastic and thermoset, mainly due to its high thermal and chemical resistance and mechanical strength. These outstanding properties can be attributed to its chemical structure, composed of phenyl groups linked by a sulfur atom, which gives rigidity to the chain. However, the low glass transition temperature and brittleness with low elongational strain also restrict its further applications.<sup>1,2</sup> Several techniques have been applied to improve those physical properties of PPS. One approach is to use glass fiber/mineral as fillers to manufacture the PPS composites with high performance.<sup>3–6</sup> Another approach, blending semicrystalline PPS with other polymers, is also proved to be an effective way of improving properties such as impact strength and toughness.<sup>7</sup>

A large number of polymers, such as thermotropic liquid crystalline polymer (TLCP),<sup>8–10</sup> poly(ethylene terephthalate) (PET),<sup>11–13</sup> polyamide (PA),<sup>14,15</sup> bisphenol A polysulfone (PSF),<sup>16</sup> poly(ether ether ketone) (PEEK),<sup>17</sup> Polypropylene (PP),<sup>18</sup> high density polyethylene (HDPE),<sup>13</sup> polycarbonate (PC),<sup>19</sup> ABS resin,<sup>20</sup> SEBS resin,<sup>21</sup> and so on, have been used to blend with PPS to obtain new polymeric materials with desirable properties in the past decades. The mechanical and physical properties of those blends have also been widely studied. The results reveal that the addition of different polymers, semicrystalline thermoplastic and amorphous thermoplastic as well as thermoplastic elastomer, has a different effect on the properties of PPS.

It is well accepted that the mechanical and physical properties of the crystalline polymers are governed by the supermolecular morphology, which in turn is controlled by the crystallization process. The properties of semicrystalline polymers such as PPS depend on the crystallization behavior of the polymer. Hence the study of the kinetics of crystallization is necessary for optimizing the process conditions and establishing the structure-property correlations in polymers. Hitherto, the crystallization behavior of neat PPS<sup>22–24</sup> and of those PPS/semicrystalline thermoplastic blends<sup>9,10,11–14</sup> has been investigated extensively by both isothermal and nonisothermal methods. For those PPS/amorphous thermoplastic blends,<sup>16,19</sup> however, the studies mainly

Correspondence to: D. Wu (dfwu@yzu.edu.cn).

Contract grant sponsor: National Natural Science Foundation of China; contract grant number: 50373034.

Contract grant sponsor: Foundation of Jiangsu Provincial Key Program of Physical Chemistry (Yangzhou University).

*Journal of Applied Polymer Science*, Vol. 105, 739–748 (2007)  
© 2007 Wiley Periodicals, Inc.

focus on the thermal and morphological properties. The crystallization kinetics of PPS in those blends hence needs to be further investigated to optimize composition-property correlations.

The amorphous PC has been chosen to blend with PPS because of its high toughness and high glass transition temperature. Lim et al.<sup>19</sup> have prepared the immiscible PPS/PC blend and investigated its thermal properties such as melting temperature and crystallization temperature as well as heat of fusion. They observed an increase of crystallinity of PPS in the blend in contrast to neat PPS. In our study, the amorphous PC was also chosen to prepare a partially miscible PPS/PC blend. The effect of PC contents on the morphology and nonisothermal crystallization behavior of blend were discussed. The crystallization kinetics was then further investigated, aiming at establishing the structure-property correlations in the PPS/PC blend.

## EXPERIMENTAL

### Material preparation

Poly(phenylene sulfide) (PPS, sieved through 40 mesh/in.<sup>2</sup>, number average molecular weight of 2100 g/mol) used in this study was obtained from Deyang Sci and Tech, P. R. China. The bisphenol A polycarbonate (PC, 201-10) is a commercial product of LG-DOW Chemical, USA. All the materials were dried at 110°C under vacuum for 6 h before using. PPS/PC blend were prepared by direct melt mixing in a rheometer (HAAKE polylab, Thermo Electron, USA) at 290°C and 50 rpm for 8 min, and the weight ratio of blends were 100/0, 80/20, 60/40, 50/50, 40/60, 20/80, and 0/100, respectively. All the blends were compression molded into sheet samples of about 1 mm in thickness for further characterization.

### Scanning electron microscope characterization

The morphologies of the fractured surfaces of the samples were investigated using a PHILIPS XL-30ESEM scanning electron microscope (SEM) with 20 kV accelerating voltage. The sheet samples were kept in liquid nitrogen and then brittle fractured. An SPI sputter coater was used to coat the fractured surfaces with gold for enhanced conductivity.

### Dynamic mechanic thermal analysis

The dynamic mechanical properties of PPS/PC blend were determined using a DMA-242C dynamic mechanical thermal analyzer (NETZSCH, USA). The testing was performed in three-point bending mode at a vibration frequency of 5 Hz in the temperature

range from 0 to 200°C at a heating rate of 5°C/min under N<sub>2</sub> atmosphere.

### Linear rheological measurements

Linear rheological measurements were carried out on a HAAKE Rheo-Stress-600 rheometer (Thermo Electron, USA) equipped with a parallel plate geometry using 15 mm diameter plates. All measurements were performed with a 200 FRTN1 transducer with a lower resolution limit of 0.02 g/cm. In the tests, the small amplitude oscillatory shear (SAOS) was applied, and the dynamic frequency scan measurements were carried out. All the sweeps were conducted at the strain of 5%.

### Polarized optical microscope characterization

The crystallization morphology of neat PPS and PPS/PC film samples were studied using a polarized optical microscope (POM, LEICA BX51) equipped with a hot stage (Linklam LTM350). The same temperature ramps were used as in DSC testing. The film samples were prepared by pressing the film between two cover glasses at 300°C using a hot plate.

### Nonisothermal crystallization process

Nonisothermal crystallization was carried out on a NETZSCH DSC-204F1 differential scanning calorimeter (DSC). The samples about 5 mg in weight for DSC were cut from the film. In the nonisothermal crystallization process, the samples were melted at 300°C for 10 min to eliminate the previous thermal history and then cooled at constant cooling rates of 5, 10, 20, and 40°C/min. The exothermal curves of heat flow as a function of temperature were recorded to analyze the nonisothermal crystallization process of the PPS and PPS/PC blends. All the experiments were carried out under nitrogen.

## RESULTS AND DISCUSSION

### Morphology of PPS/PC Blends

A morphological study was carried out on the PPS/PC blend using SEM. Figure 1 gives the images of the fracture surface of blends in various compositions. It is hard to observe the obvious phase separation between two components almost in all blends, which is different from that reported by Lim et al.<sup>19</sup> They find that PPS/PC blend has a remarkable immiscible morphology, showing the typical dispersed phase/matrix structure.

The dynamic mechanical thermal analysis (DMTA) may give more information on the phase structure of PPS/PC blend. The tan  $\delta$  curves of the blends are

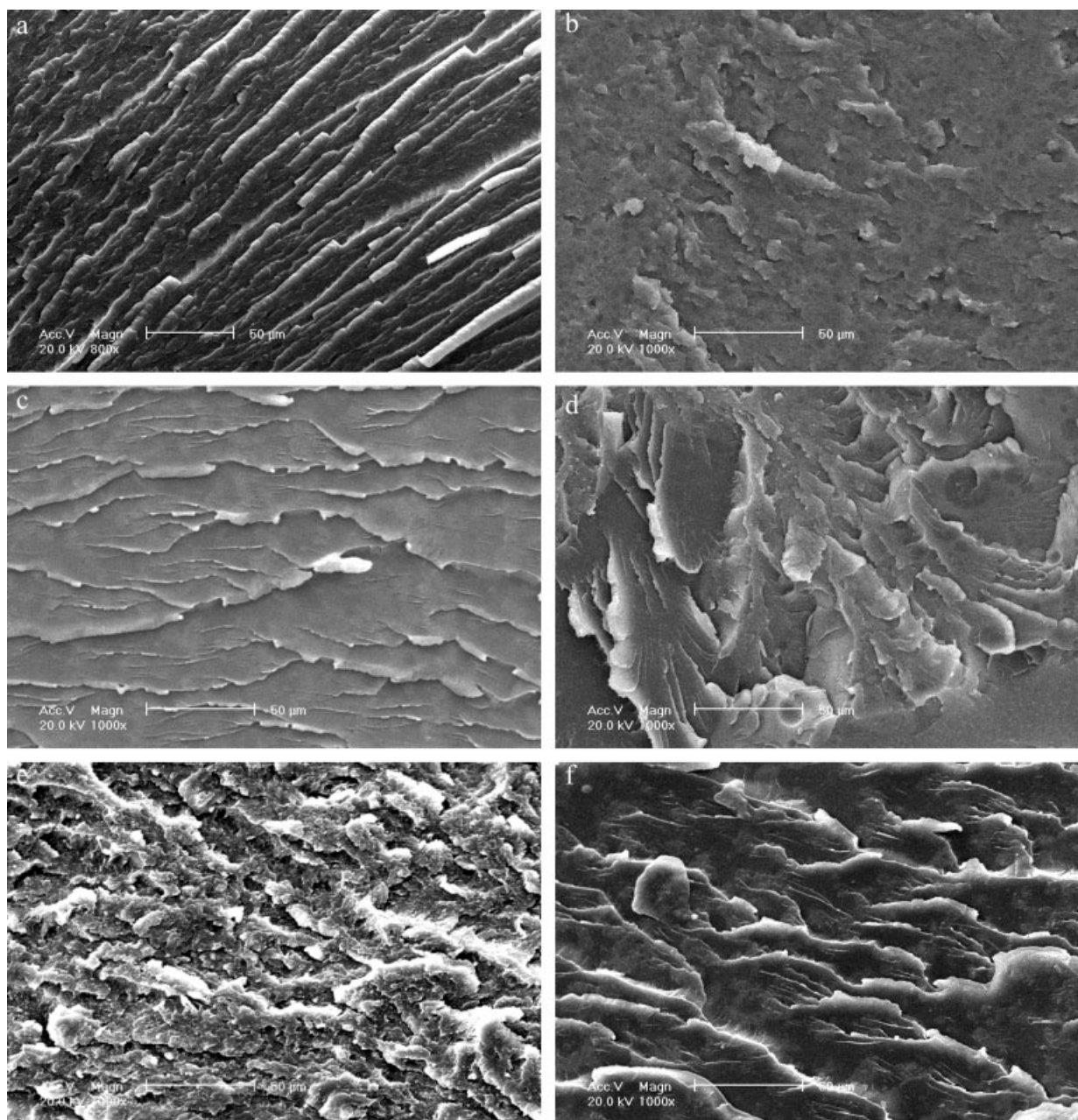


**Figure 1** SEM images of PPS/PC blends in composition of (a) 100/0, (b) 80/20, (c) 60/40, (d) 50/50, (e) 40/60, and (f) 20/80.

represented in Figure 2 to compare the glass transition temperature ( $T_g$ ) of each component. It can be observed that with addition of PC component, the  $T_g$  increases from about 128 to 136°C for PPS phase and decreases from about 160 to 148°C for PC phase. Clearly, the two peaks of  $\tan \delta$  shift close to each other to some extent in contrast to that of neat PPS and PC, suggesting a possible partial miscibility of the PPS/PC blend. The increasing  $T_g$  of PPS component and decreasing  $T_g$  of PC component can be attributed to the changes of phase morphology and crystallization behavior as well as viscoelastic prop-

erties of the blend, which will be discussed in the later corresponding sections. Same change of  $T_g$  has also been observed in the partially miscible PMMA/PC blend.<sup>25</sup> Yoon and White<sup>7</sup> examined the interfacial tension of PPS with other polymer melts and reported the order of the interfacial tensions of PPS with other polymers as PPS/PA6 > PPS/PE > PPS/PP  $\approx$  PPS/PET > PPS/PC > PPS/PS > PPS/PSF. The presence of such local ordering also indicates that the PPS and PC components in the blends are compatible somewhat to each other because of their analogous chemical structure. The relative lower

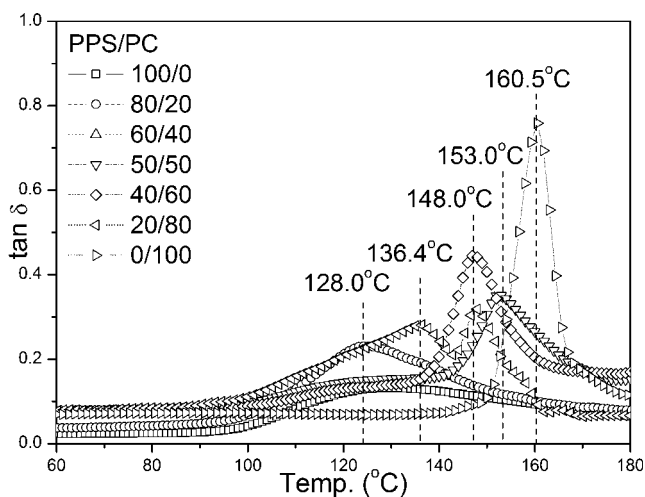


**Figure 2** DMTA thermogram at 5 Hz of PPS/PC blends.

interfacial tensions therefore indicate that the phase interface in the PPS/PC blend may be illegible, which is not easy to be observed directly.

Recently, rheometry has been recognized as a powerful tool for investigating the internal structure of multiphase polymer systems. For the immiscible and/or partially miscible polymer blend, the rheological behavior depends (among other things) on the compatibility and deformability of the discrete phase strongly. Phase inversion, droplet shape, cocontinuity, and conversion of droplets into fibrils with different degrees of alignment depending on stress level are all parameters that have been suggested to be responsible for the special rheological responses.<sup>26–32</sup>

Figure 3 gives the storage modulus ( $G'$ ) and complex viscosity ( $\eta^*$ ) for PPS/PC blend obtained from the SAOS measurements. The linear viscoelastic region, strain of 5%, was firstly determined by the dynamic strain sweep. On Figure 3(a), it is clear when compared with pristine PPS, the low-frequency storage modulus of the blend increases monotonically with the content of PC up to 60 wt %. This decrease of frequency dependency can attribute to the phase separation.<sup>26–28</sup> It is also notable that almost all the blends show a weak modulus plateau at the frequency region of about 0.1–1 Hz. (See the arrows) Utracki<sup>33</sup> points out that this moderate-frequency plateau is attributed to the shape relaxation of dispersed domain in polymer blend system because the relaxation time of this behavior is generally in the order of  $10^0$ – $10^1$  s. It further suggests that the dispersed PC domain/PPS matrix morphology does exist despite of partial miscibility of the blends. Therefore, the interfacial area between the continuous PPS and the dispersed PC domains increases with increase of PC content, enhancing the elastic responses of blends. Also as a result, the blends

reveal the stronger shear-thinning behavior in comparison with neat PPS and PC, as can be seen in Figure 3(b).

However,  $G'$  of 20/80 blend decreases remarkably in contrast to that of 40/60 blend, although still higher than neat PC. It indicates that the phase in this blend may be converted from PC domain to PPS domain. According to Paul and Backnall,<sup>34</sup> the condition for phase inversion is expressed by:

$$\frac{\eta_1}{\eta_2} = \frac{\phi_1}{\phi_2} \quad (1)$$

where  $\phi_i$  and  $\eta_i$  are the volume fraction and melt viscosity of component  $i$ . For the PPS/PC blend, basing on low-frequency viscosity of PPS (142 Pa s) and PC (313 Pa s) obtained from Figure 3(b), the calculated phase inversion point is near the weight ratio of about 35/65. Therefore, the phase structure of blend 20/80 may reverse from those blends in rich PPS component.

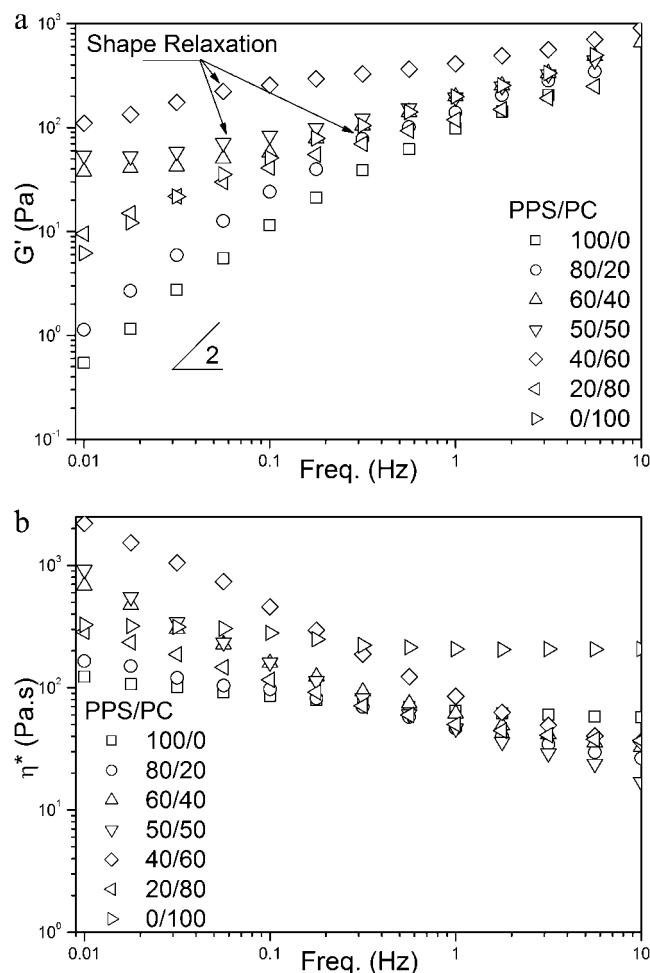


**Figure 3** Rheological curves of (a) storage module and (b) complex viscosity for PPS/PC blends in SAOS measurements.



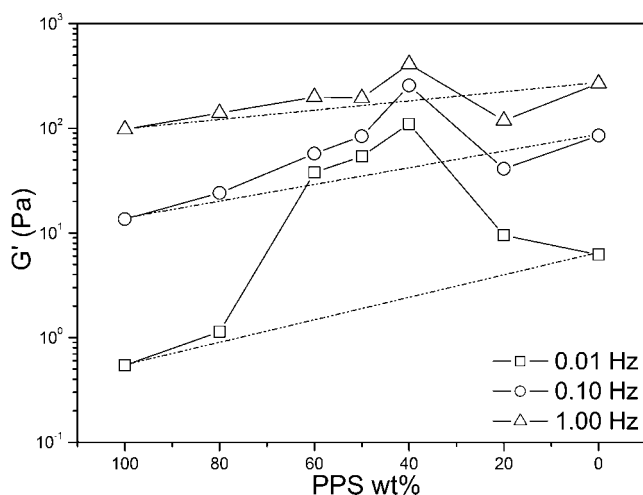


**Figure 4** Plots of dynamic storage module as a function of blend composition for the PPS/PC blends at various frequencies.

Utracki<sup>33</sup> consider that the viscoelastic functions for the miscible blends usually follow the log-additivity rule

$$\log F_b = \omega_m \log F_m + \omega_d \log F_d \quad (2)$$

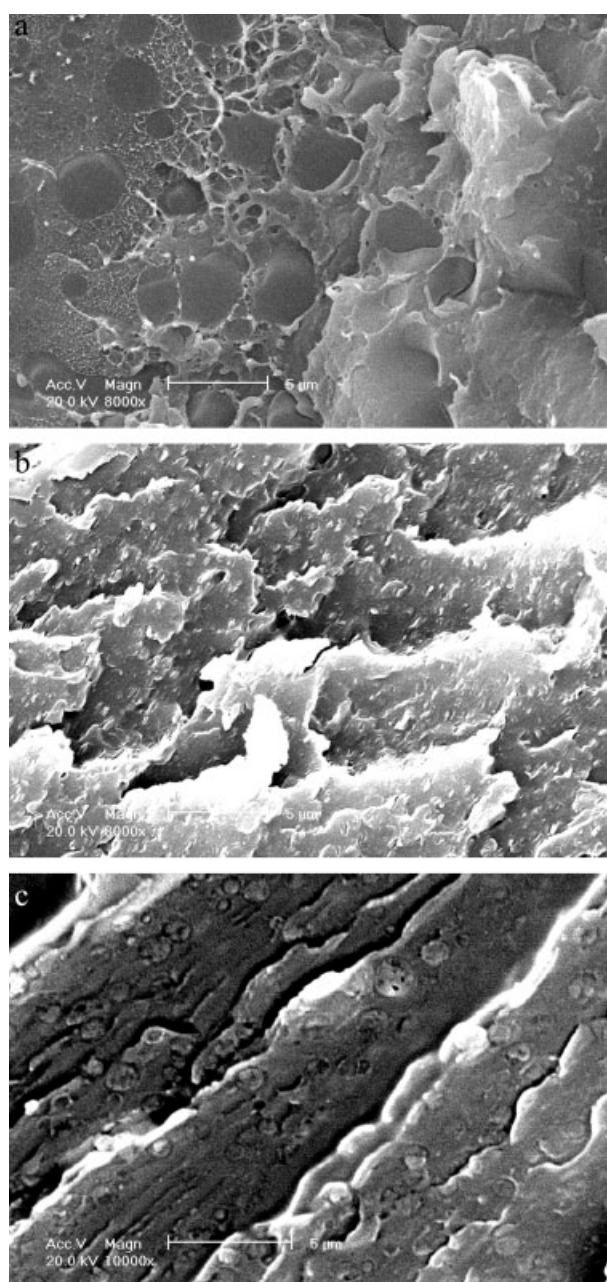
where  $F$  is a viscoelastic function;  $w$  is the weight fraction; and subscripts  $b$ ,  $m$ , and  $d$  indicate the values for the blend, the matrix, and the dispersed phase, respectively. However, the viscoelastic functions for the immiscible blends usually deviate from the log-additivity rule, showing positive deviation, negative deviation, and positive-negative deviation, which depends on the blend-composition dependence of the viscoelastic functions.<sup>35,36</sup>

Figure 4 gives the composition dependence of  $G'$  at different frequencies for PPS/PC blends. Obviously, the modulus-composition curves reveal an S shape and  $G'$  shows positive-negative deviation from the log-additivity rule. Two possible explanations for this positive-negative deviation have suggested by Utracki and Favis<sup>37</sup>: partial miscibility at low concentration and concentration-dependent change of the flow mechanism in the immiscible region. Thus, the rheological behavior observed confirms the partial miscibility behavior of PPS/PC blends.

Furthermore, Han<sup>38</sup> has attributed this positive-negative deviation behavior of polymer blends to a phase inversion at a certain blending ratio identified by the point of transition of the curves. On Figure 4,  $G'$  (1 Hz) of the PPS/PC blends shows positive deviation in the PPS contents between 100 and 40 wt %, whereas negative deviation occurs for PPS contents less than 30 wt %. It indicates that phase inversion occurs at PPS contents between 40 and 30 wt %

in the blend, which is in agreement with the calculated result from formula (1).

Those results from rheological behaviors are further confirmed by SEM measurements. Figure 5 displays the SEM photographs in high magnification for the blends. It can be observed that the dispersed domain/matrix morphology exists both in the blends of 80/20 and 20/80 (See the arrows). In the 80/20 blend, the PC droplet shows an average size of about 3–4  $\mu\text{m}$  [Fig. 5(a)], while the PPS droplet in the 20/80 blend is less than 1  $\mu\text{m}$  because of its lower viscosity than PC matrix [Fig. 5(c)].<sup>33</sup> Both of



**Figure 5** SEM images of PPS/PC blends in composition of (a) 80/20, (b) 40/60, and (c) 20/80.

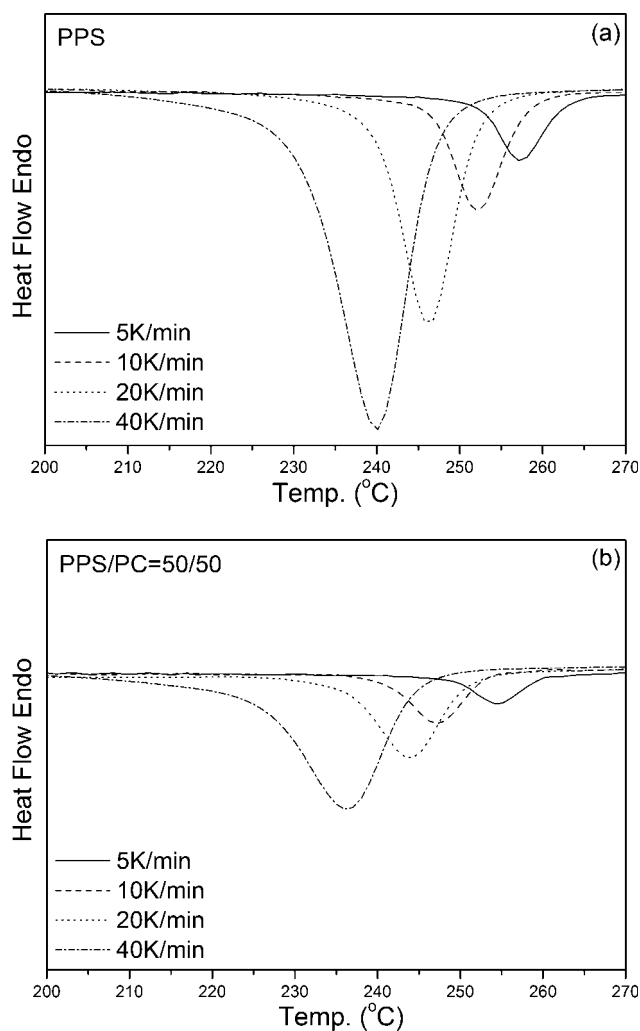


**Figure 6** The heat flow curves at various cooling rates for (a) pure PPS and (b) PPS/PC blend.

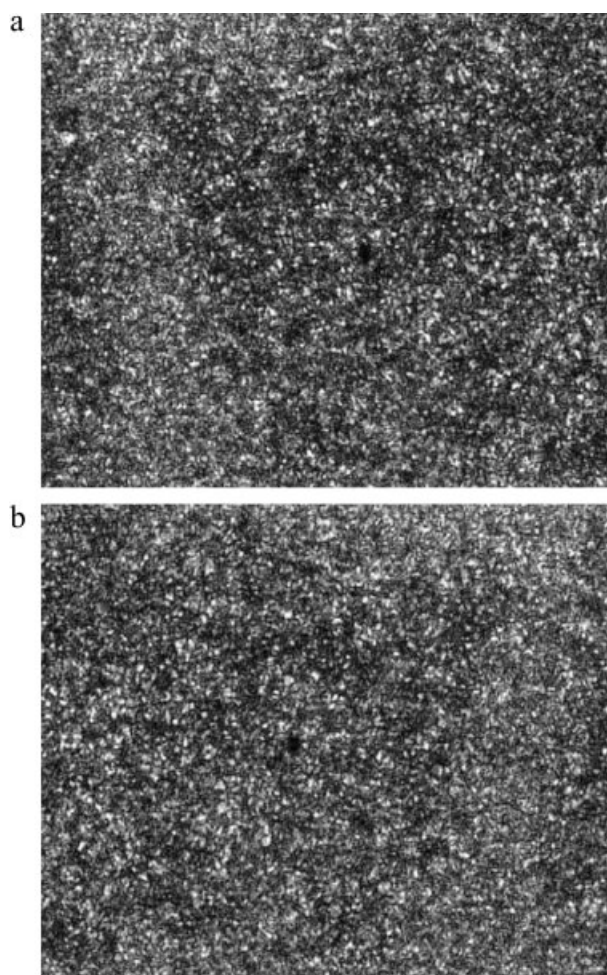
these two blends reveal an illegible phase interface structure, however, illuminating the partial miscibility between PPS and PC. The phase morphology of the 40/60 blend is far more complex than the blends of 80/20 and 20/80, as showed in Figures 5(b) and 1(e). One possible reason is that the weight ratio of 40/60 is close to phase inversion region. The detailed phase inversion behavior of PPS/PC blend will be discussed in another paper.

Therefore, the addition of amorphous component, PC, to PPS leads to the formation of three different phase morphologies in the PPS/PC blend: dispersed PPS/continuous PC (80/20), dispersed PC/continuous PC (20/80), and complex morphology (40/60). Since the contents of PC component have influences on the morphology, it may also influence the crystallization behavior of blend, too. The following measurements on the nonisothermal crystallization behavior are mainly carried out around those three blends and neat PPS.

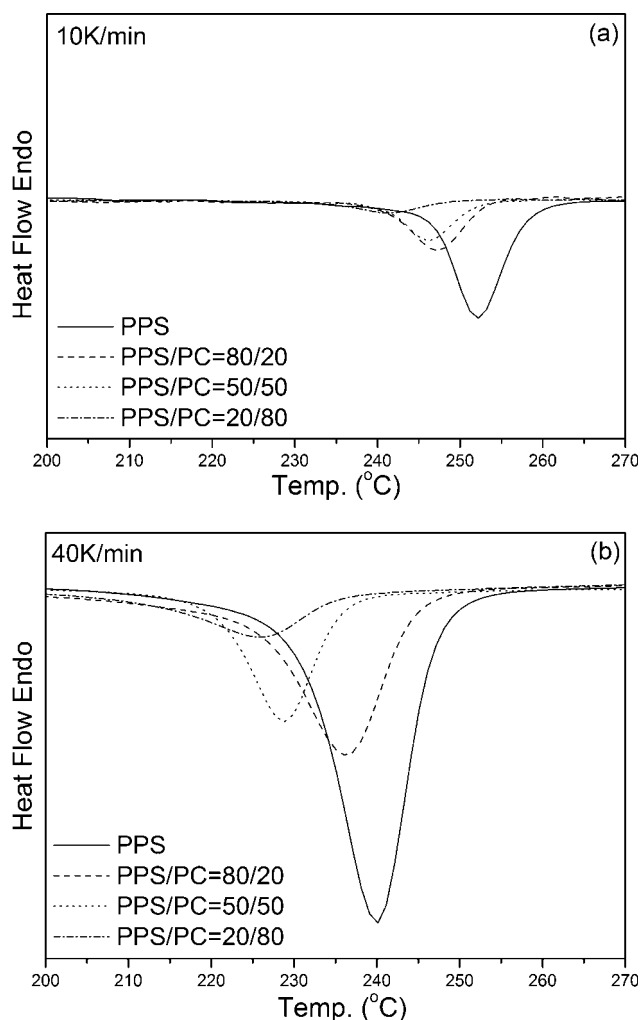
### Nonisothermal crystallization behavior

Figure 6 gives the nonisothermal crystallization curves at different cooling rates for neat PPS and its blend. With increase of the cooling rate, the exothermic peak of both neat PPS and blend shift to low temperatures and, the exotherms broaden gradually. It is noteworthy that the exothermic peak intensity of the blend decreases in contrast to that of neat PPS [comparison between Fig. 6(a,b)], which suggests that the addition of amorphous PC component may have influence on the nonisothermal crystallization behavior of PPS. Figure 7 gives the POM observation of neat PPS and its blend. The grainy structure seen on the micrograph represents spherulites. However, it is difficult to directly observe the effect of PC on the spherulites structure of PPS matrix because both of these two samples show the small spherulites sizes after nonisothermal crystallization, which are out of the range for POM experiment.

Figure 8 gives the nonisothermal crystallization curves at identical cooling rates for all blends.



**Figure 7** POM images of (a) neat PPS and (b) PPS/PC 40/60 blend.



**Figure 8** The heat flow curves for PPS/PC blends at the cooling rates of (a) 10°C/min and (b) 40°C/min.

Clearly, the presence of PC and/or partial miscible morphology of blend have remarkable influence on the crystallization of PPS matrix. The exothermic peak of PPS shifts to low temperatures gradually with increase of the PC contents whatever at high or low cooling rates and, the exothermic peak intensity also decreases monotonously. It suggests that in the PPS/PC blend, the amorphous PC may act as a role of inhibitor to the crystallization of PPS. Similar phenomenon has also been observed in PPS/LCP blend by Budgell and Day.<sup>22</sup>

However, for most of PPS blends, especially for those PPS/semicrystalline polymer blends such as PPS/PA,<sup>14</sup> PPS/PEEK,<sup>18</sup> and PPS/TLCP,<sup>9,10</sup> it has been found that the second polymer component can serve as a heterogeneous nucleation agent, promoting crystallization of PPS despite of the compositions of blend. As a result, the PPS component in the blend usually shows higher crystallization temperatures than that of neat PPS. But Gopakumar et al.<sup>10</sup> have observed in PPS/TLCP blend that the crystallization

rate of PPS phase increases with the TLCP content to 30 wt % while decreases on further addition for melt-mixed blends, which is different from that of coprecipitated blend. They hence attribute this behavior to the extent of phase separation between two phases in the blend. Similar trend in the crystallization behavior of PPS/PET blend has also been reported by Hanley et al.<sup>12</sup>

### Nonisothermal crystallization kinetics

Therefore, to further investigate the effect of amorphous PC component on the crystallization behavior of PPS in the PPS/PC blend, the nonisothermal crystallization kinetics of neat PPS and its blends were compared. Avrami equation was used to directly analyze the nonisothermal crystallization process.<sup>39</sup>

$$X(t) = 1 - \exp(-Kt^n) \quad (3)$$

$$\log[-\ln(1 - X(t))] = n \log t + \log K \quad (4)$$

where  $X(t)$  is relative crystallinity at crystallization time,  $t$ ,  $n$  is the Avrami exponent,  $K$  is the crystallization rate constant changed with temperature. Figure 9 shows a typical relative crystallinity curves for neat PPS and blend. The corresponding Avrami plots eq. (4) are shown in Figure 10. Two different regions can be observed: a linear one and a gentle "roll-off." The "roll-off," which is attributed to secondary crystallization, cannot be analyzed by the Avrami theory. Therefore, from the linear region of this plot,  $n$  and  $k$ , can be calculated.

Considering the effect of the various cooling rate on the nonisothermal crystallization process, the final form of the parameter characterizing kinetics during nonisothermal crystallization were given by Jeziorny:<sup>40</sup>

$$\ln Z_c = \ln Z_t / \phi \quad (5)$$

where  $Z_t$  is the crystallization rate constant,  $Z_c$  is the modified crystallization rate constant considering cooling rate,  $\phi$ . The results obtained from Avrami plots and Jeziorny methods were listed in Table I. It can be observed that pure PPS gives a value of about  $2.8 < n < 3.1$ . This value is in accordance with that reported in the literatures, suggesting that the nucleated process of pure PPS lead to a spherical three-dimensional growth with thermal nucleation.<sup>22-24</sup>

In the case of PPS/PC blend, the value of Avrami exponent decreases more or less. Two factors may lower the value of Avrami exponent,  $n$ : (1) fast crystallization rate of the blend systems at lower temperatures prevents the spherulite from developing into three-dimensional crystallites; (2) growth site

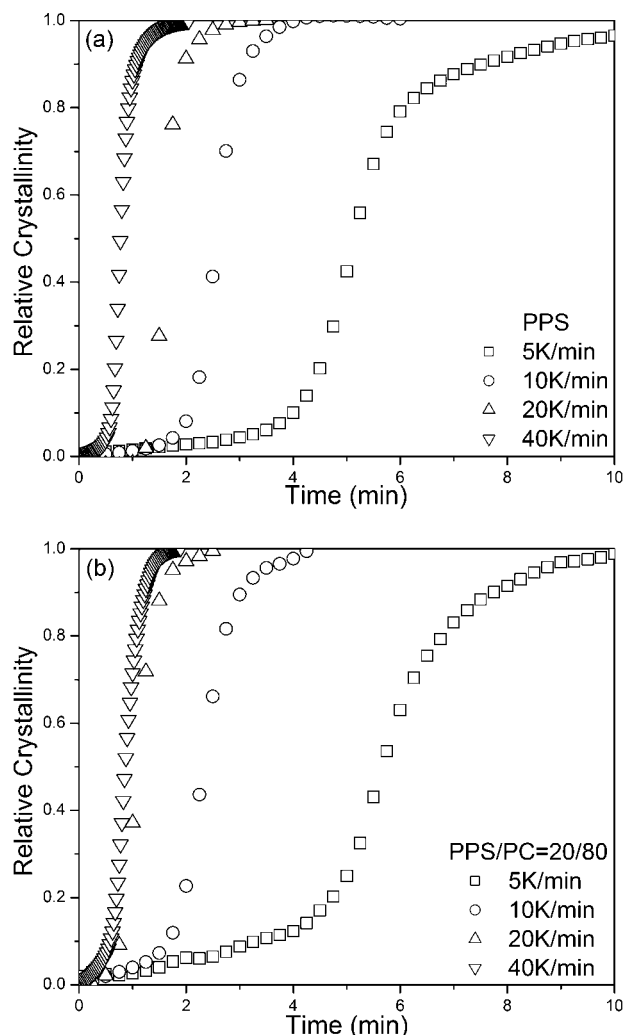


**Figure 9** The curves of relative crystallinity versus temperature at various cooling rates for (a) pure PPS and (b) PPS/PC blend.

impingement truncation of spherulites, impurity segregation, and slightly slow secondary crystallization may change the crystallization mechanism if the crystalline weight fraction is higher than 0.5.<sup>10,24</sup> Compared with those of PPS/PA6, PPS/TLCP blends,<sup>9,14</sup> the decrease of the value of Avrami exponent for the PPS/PC blend is very small, however, suggesting that the presence of amorphous component, PC, only has a little heterogeneous nucleation effect on the crystallization of PPS in the blend. Similar phenomenon in PPS/PET blend has also been reported by Shangankuli et al.<sup>6,11</sup> They observe that the nucleation of PPS in a nonisothermal crystallization is unaffected by the presence of PET.

It is well known that in the polymer blends the thermal and chemical environment under which a polymer crystallizes is modified as a result of the presence of the second component. The critical factors governing the extent and direction of change

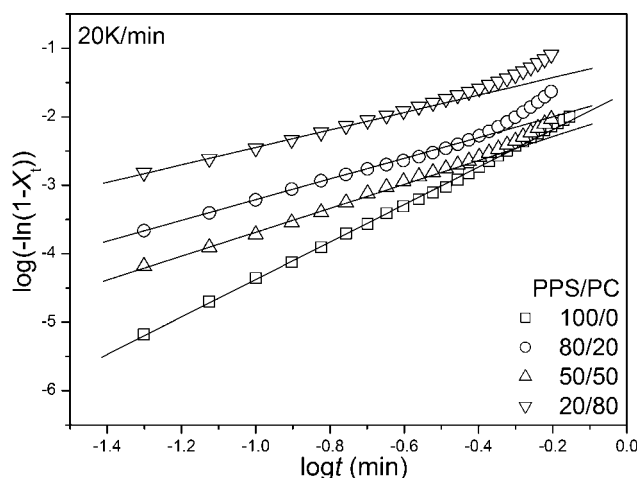


**Figure 10** Plots of  $\log[-\ln(1 - X(T))]$  versus  $\log t$  at the cooling rate of 20°C/min.

in the overall crystallization rate and crystallization temperature of two components include miscibility, relative melt viscosities, chemical compatibility, amounts of the component polymers, and their phase morphology.<sup>13</sup> Mai et al.<sup>14</sup> have observed in the immiscible PPS/PA6 blend that PA6 phase has strong heterogeneous nucleation effect and, the possibility of interfacial interactions in the blends also lead to an increase in the local ordering of the PPS chains in the molten state of the blends because of the higher interfacial tension for the PPS/PA6 blend.

For the PPS/PC blend, as mentioned in the section of morphology studies, the PPS and PC components present a partial miscibility of the blend. Although phase separation still presents in the blend, the phase interface is very illegible. The heterogeneous nucleation effect on the crystallization of PPS by amorphous PC phase and/or phase interface is hence

**TABLE I**  
Parameters from the Avrami and Jeziorny as Well as Kissinger Method

PPS/PC	$\phi$ (K/min)	$n$	$Z_c$	$\Delta E$ (kJ/mol)
100/0	5	3.11	0.631	62.4
	10	2.92	0.695	
	20	2.83	0.982	
	40	2.79	1.202	
80/20	5	2.88	0.602	64.6
	10	2.70	0.615	
	20	2.38	0.838	
	40	2.27	1.052	
40/60	5	2.91	0.549	70.2
	10	2.75	0.628	
	20	2.45	0.810	
	40	2.32	0.958	
20/80	5	2.74	0.358	72.6
	10	2.61	0.552	
	20	2.36	0.795	
	40	1.98	0.954	



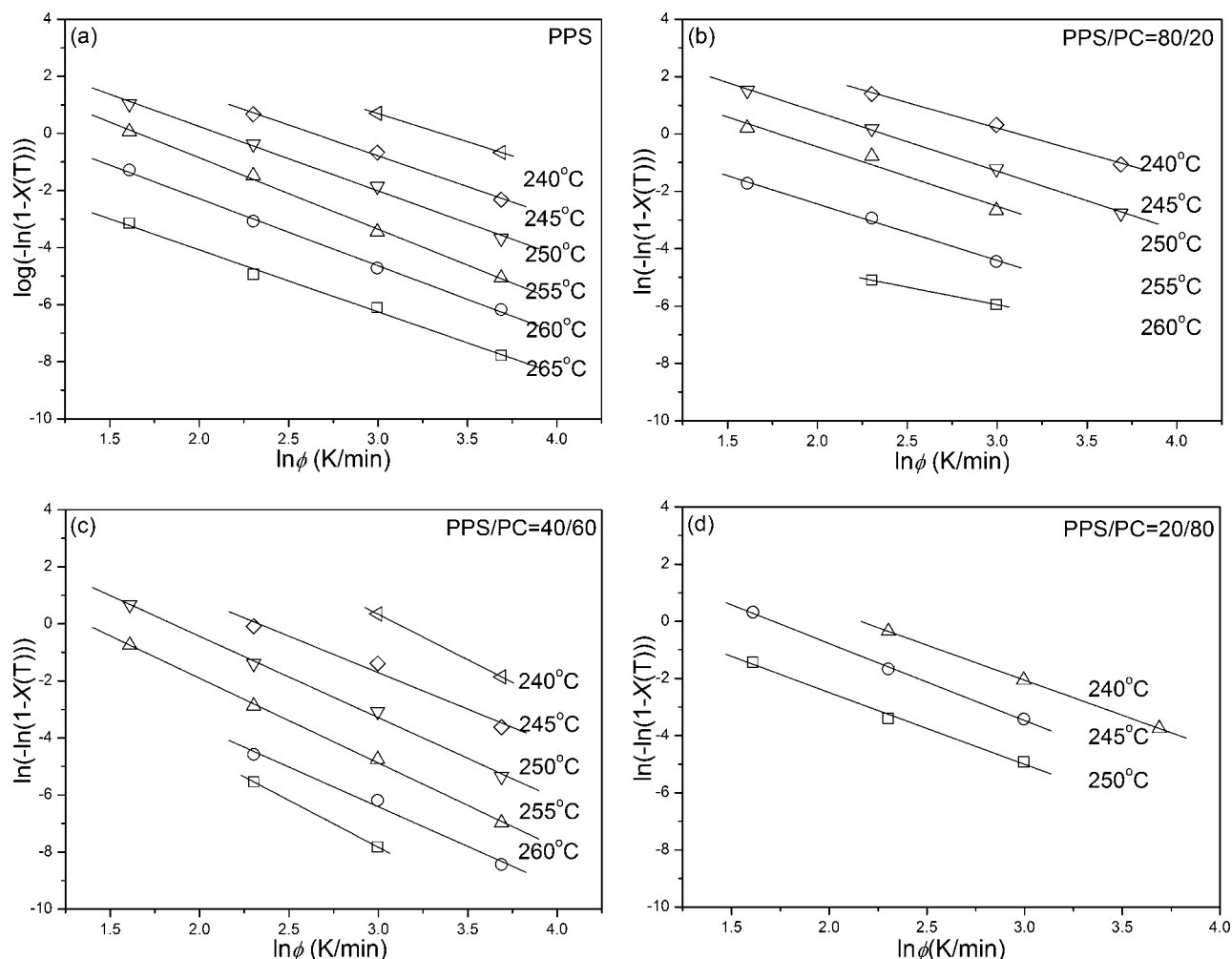


**Figure 11** Plots of  $\ln[-\ln(1 - X(T))]$  versus  $\ln \phi$  for (a) pure PPS and the blend of (b) 80/20, (c) 40/60, and (d) 20/80.

not remarkable. On the other hand, the viscosity of blend increases sharply with addition of PC component [See Fig. 3(b)], which will lower the chain mobility of PPS. Therefore, the presence of amorphous PC phase inhibits PPS phase from crystallization to some extent, causing a slow crystallization of the blend in contrast to that of pure PPS, which is suggested also by the decreasing value of crystallization rate constant listed in Table I.

Ozawa<sup>41</sup> developed the Avrami method to deal with the nonisothermal crystallization process. Presuming that the nonisothermal crystallization process is composed of many infinitesimal isothermal one, the kinetics equation can be described as follows:

$$X(T) = 1 - \exp(-K(T)/\phi^m) \quad (6)$$

$$\ln[-\ln(1 - X(T))] = \ln K(T) - m \ln \phi \quad (7)$$

where  $X(T)$  is a cooling function,  $m$  is the Ozawa exponent,  $\phi$  is cooling rate. Plots of  $\log t$  versus  $\ln \phi$  for the pure PPS and its blends are shown in

Figure 11. The nice linearity of those curves suggests that the Ozawa model may provide a satisfactory description to the nonisothermal crystallization for both the pure PPS and its blends. This validity of Ozawa equation has been also observed in PPS/TLCP blends.<sup>10</sup> But it is notable that the temperatures region of this validity reduces with increasing of PC contents, also indicating a content dependence of the hindrance effect by PC.

Kissinger<sup>42</sup> has suggested a method to determine the activation energy for the transport of the macromolecular segments to the growing surface,  $\Delta E$ , by calculating the variation of  $T_p$  with the cooling rate  $\phi$ :

$$\frac{d[\ln(\phi/T_p^2)]}{d(1/T_p)} = \frac{-\Delta E}{R} \quad (8)$$

where  $R$  is the gas constant. The value of  $\Delta E$  is also listed in Table I. Clearly,  $\Delta E$  of the PPS/PC blend increases monotonously, with increase of PC contents. It indicates that presence of PC phase in the blend impedes the transport of PPS chain segments

to the growing surface to some extent during crystallization process, which may be attribute to the higher viscosity of PC component and/or its partial miscibility with PPS phase. Those results hence further confirm that the amorphous PC may act as a crystallization inhibitor of PPS in the partial miscible PPS/PC blend.

### CONCLUSIONS

Investigations on the morphology and nonisothermal crystallization kinetics were carried out on PPS/PC blend prepared by melt mixing. The results reveal that the blend is partially miscible due to the nice compatibility between two components, although the illegible phase separation can still be observed. With the addition of amorphous PC, the crystallization temperatures of PPS decrease with increasing of PC contents. The heterogeneous nucleation effect by amorphous PC phase and/or phase interface is not remarkable. On the contrary, the increasing of viscosity due to the addition of PC results in the decreasing of crystallization rate of PPS in the blend. Therefore, the presence of PC phase inhibits PPS phase from crystallization to some extent.

### References

- Chawla, K. K. *Composites Materials (Materials Research and Engineering Series)*; Springer: New York, 1987.
- Fried, J. R. *Polymer Science and Technology*, 2nd ed.; Pearson Education: New York, 2003.
- Garrell, G. M.; Ma, B. M.; Shih, A. J.; Curzio, E. L.; Scattergood, R. O. *Mater Sci Eng A* 2003, 359, 375.
- Sinmazcelik, T. *Mater Des* 2006, 27, 270.
- Lu, D.; Mai, Y. W.; Robert, K.; Li, Y.; Ye, L. *Macromol Mater Eng* 2003, 288, 693.
- Shangankuli, V. L.; Jog, J. P.; Nadkani, V. M. *J Appl Polym Sci* 1988, 36, 335.
- Yoon, P. J.; White, J. L. *J Appl Polym Sci* 1994, 51, 1515.
- Han, M.; Kim, W. N.; Giles, D. W. *Polym Eng Sci* 2001, 41, 1506.
- Gabellini, G.; Bretas, R. E. S. *J Appl Polym Sci* 1996, 61, 1803.
- Gopakumar, T. G.; Ghadage, R. S.; Ponrathnam, S.; Rajan, C. R.; Fradet, A. *Polymer* 1997, 38, 2209.
- Shangankuli, V. L.; Jog, J. P.; Nadkani, V. M. *J Appl Polym Sci* 1994, 51, 1463.
- Hanley, S. J.; Nesheiwat, A. M.; Chen, R. T.; Jamieson, M.; Pearson, R. A.; Sperling, L. H. *J Polym Sci Part B: Polym Phys* 2000, 38, 599.
- Jog, J. P.; Shangankuli, L.; Nadkani, V. M. *Polymer* 1993, 34, 1966.
- Mai, K.; Zhang, S.; Zeng, M. *J Appl Polym Sci* 1999, 74, 3033.
- Chen, Z.; Li, T.; Yang, Y.; Liu, X.; Lu, R. *Wear* 2004, 257, 696.
- Mai, K.; Mei, Z.; Xu, J.; Zeng, H. *J Appl Polym Sci* 1998, 69, 637.
- Mai, K.; Mei, Z.; Xu, J.; Zeng, H. *J Appl Polym Sci* 1997, 63, 1001.
- Quan, H.; Zhong, G. J.; Li, M. Z.; Yang, M. B.; Xie, B. H. *Polym Eng Sci* 2005, 45, 1303.
- Lim, S.; Kim, J.; Park, M.; Choe, C. R.; Lee, J.; Kim, D. *Polym Eng Sci* 1996, 36, 2502.
- Nam, J. D.; Kim, J. Y.; Lee, S.; Lee, Y.; Park, C. *J Appl Polym Sci* 2003, 87, 661.
- Hisamatsu, T.; Nakano, S.; Adachi, T.; Ishikawa, M.; Iwakura, K. *Polymer* 2000, 41, 4803.
- Budgell, D. R.; Day, M. *Polym Eng Sci* 1991, 31, 1271.
- Lopez, L. C.; Wilkes, G. L. *Polymer* 1988, 29, 106.
- Lopez, L. C.; Wilkes, G. L. *Polymer* 1989, 30, 147.
- Kim, W. N.; Burns, C. M. *Macromolecules* 1987, 20, 1876.
- Li, R. M.; Yu, W.; Zhou, C. X. *Polym Bull* 2006, 56, 455.
- Yavari, A.; Asadinezhad, A.; Jafari, S. H.; Khonakdar, H. A.; Ahmadian, A.; Bohme, F. *Macromol Mater Eng* 2005, 290, 1091.
- Kitade, S.; Takahashi, Y.; Noda, I. *Macromolecules* 1994, 27, 7397.
- Nandan, B.; Kandpal, L. D.; Mathur, G. N. *J Polym Sci Part B: Polym Phys* 2004, 42, 1548.
- Steinmann, S.; Gronski, W.; Friedrich, C. *Polymer* 2001, 42, 6619.
- Weis, C.; Leukel, C.; Borkenstein, K.; Maier, D.; Gronski, W.; Friedrich, C.; Honerkamp, J. *Polym Bull* 1998, 40, 235.
- Utracki, L. A. In *Current Topics in Polymer Science*; Ottenbrite, R. M.; Utracki, L. A.; Inoue, S., Eds.; Hanser: Munich, 1987; Vol. II.
- Utracki, L. A. *Polymer Blends and Alloys: Thermodynamics and Rheology*; Hanser: New York, 1989.
- Paul, D. R.; Bucknall, C. B., Eds.; *Polymer Blends: Formulation and Performance*; Wiley: New York, 2000.
- Utracki, L. A.; Kamal, M. R. *Polym Eng Sci* 1982, 22, 96.
- Utracki, L. A. *Polym Eng Sci* 1983, 23, 602.
- Utracki, L. A.; Favis, B. D. In *Handbook of Polymer Science and Technology*; Cheremisinoff, N. P., Ed.; Marcel Dekker: New York, 1989; p 156.
- Han, C. D. *Multiphase Flow in Polymer Processing*; Academic Press: New York, 1981; Chapter 4.
- Avrami, M. *J Chem Phys* 1939, 7, 1103.
- Jeziorny, A. *Polymer* 1978, 19, 1142.
- Ozawa, T. *Polymer* 1971, 12, 150.
- Kissinger, H. *J Res Natl Bur Stand* 1956, 57, 217.